Saeed AHMAD[1,2], Raja A. RIAZ[1,2,3], Sheng CHEN[3], Ghufran SHAFIQ[1,2] , Shinya SUGIURA[4], Lajos HANZO[3]

Center for Advanced Studies in Telecommunication, CIIT Islamabad (1), COMSATS Institute of Information Technology, Islamabad (2), School of ECS, University of Southampton (3), Toyota Central Research and Development Laboratories (4)

Stability Analysis of the Linear Time-Invariant Ultra-WideBand Channel

Abstract. *The stability of a general Linear Time-Invariant (LTI) Ultra-WideBand (UWB) Channel Impulse Response (CIR) model is investigated. Since the s-domain or z-domain function of the UWB CIR has an extremely high number of singularities, it cannot be automatically guaranteed that none of the poles falls on the right-half of the s-plane or outside the unit-circle of the z-plane. Hence the stability analysis necessitates the exhaustive testing of classical stability criterion for a potentially excessive number of poles. We circumvent this arduous task by developing the closed-form time-domain response of the so-called homogenous, non-homogenous and vectorial LTI causal UWB system. Furthermore, the normalized settling time of the step response is evaluated for diverse damping coefficients. Finally, a stability case-study is provided with the aid of Nichols chart.*

Streszczenie. *Zbadano stabilność ultra szerokopasmowego kanału LTI. Ponieważ na płaszczyźnie s i z odpowiedź impulsowa ma wiele osobliwości nie można automatycznie zagwarantować, że wszystkie są w prawe połówce płaszczyzny s lub w2ewnątrz koła jednostkowego z. W pracy zaproponowano metodę określania stabilności kanału. (**Analiza stabilności ultra szerokopasmowego kanału LTI**)*

Keywords: UWB, No-Line-of-Sight, Residential, Stability.
Słowa kluczowe: kanał szeokopasmowy, stabilność, LTI.

Introduction and the Problem Statement

Ultra-WideBand (UWB) is a fast emerging technology after the Federal Communications Commission (FCC) ruling in the United States, unleashing huge bandwidth (3.1 − 10.6) GHz where UWB radios overlaying coexistent RF systems can operate using low-power ultra-short information bearing pulses [1]. These pulses based on the emission of low power and having an effective bandwidth larger than 500 MHz are being considered for the next generation of wireless short range communication systems [2]. In the recent years, UWB communication systems have attracted the attention of many disciplines including, among others, antennas and propagation, electromagnetic compatibility, electronics, and signal processing for communications.

A general Linear Time-Invariant (LTI) Ultra-WideBand (UWB) Channel Impulse Response (CIR) of the form [3] is

$$h^{(k,t)}(t) = \sum_{l=0}^{L}\sum_{k=0}^{K} b_{(k,l)} e^{j\phi_{(k,l)}} \delta(t - T_l - \tau_{(k,l)}) \tag{1}$$

considered, where $b_{(k,l)}$ is the weight of the k^{th} CIR tap in the l^{th} cluster, T_l is the delay of the l^{th} cluster, and $\tau_{(k,l)}$ is the delay of the k^{th} MultiPath Component (MPC) relative to the l^{th} tap-cluster's commencement time T_l. The phases $\phi_{(k,l)}$ are uniformly distributed, i.e., for a bandpass system the phase is assumed to be a random variable uniformly distributed in the range of [0, 2π]. The classic Saleh-Valenzuela (SV) model [4] does not specify the number of clusters occurring. Rather, it assumes that their number is theoretically infinite, and that their amplitude decreases exponentially with time; for practical purposes, an arbitrary threshold has to be introduced so that the clusters having an amplitude below that threshold are no longer considered in the simulations.

Problem Statement: The Given the nature of the UWB CIR of Eq (1), the corresponding s-domain or z-domain transfer function has an extremely high number of singularities and it cannot be automatically guaranteed that none of the poles falls on the right-half of the s-plane or outside the unit-circle of the z-plane. In this letter, we demonstrate for three specific scenarios that the LTI system described by Eq (1) retains stability.

We deviated from the conventional approach where the linear system is said to be asymptotically stable if and only if all the roots of the transcendental equation describing the CIR are on the left half of the complex s-plane. Since there are a high number of roots to be examined, the corresponding stability analysis is a complex task. We circumvent this arduous task by developing the closed-form time-domain response of the LTI system. These expressions are developed using the s-transform of the system model and the general form of the Leibniz integral rule [5]. To elaborate a little further, the normalized settling time and % overshoot of the step response provide a tangible quantitative characterization of the LTI system's stability. The corresponding derivation requires somewhat tedious algebraic manipulations but circumvents the arduous task of checking the position of a potentially excessive number of roots of the transcendental equation in the complex s-plane.

The rest of this letter is organized as follows. Section II derives the time-domain responses of both homogenous and non-homogenous systems. In Section III the stability of the so-called residential No-Line-of-Sight (NLOS) system model of [3] is analysed. The normalized settling time of the step response versus the damping coefficients is considered along with a stability case-study carried out with the aid of the classic Nichols chart [6]. Finally, Section IV provides our conclusions.

Methodology

The complex tap-values of a general LTI UWB CIR given in Eq (1) obey the standard Poisson-distribution while mixed Poissonian processes describe the number of clusters, the clusters arrival times and the ray arrival times within a specific cluster [3],

$$\begin{aligned} pdf_L(L) &= \frac{\left(\bar{L}\right)e^{-\bar{L}}}{L!} \\ \left(T_l \mid T_{l-1}\right) &= \Lambda_l e^{\left[-\Lambda_l\left(T_l - T_{l-1}\right)\right]}, l > 0 \\ p\left(\tau_{(k,l)} \mid \tau_{(k-1,l)}\right) &= \beta\lambda_1 e^{\left[-\lambda_1\left(\tau_{(k,l)} - \tau_{(k-1,l)}\right)\right]} \\ &\quad + \left(1-\beta\right)\lambda_2 e^{\left[-\lambda_2\left(\tau_{(k,l)} - \tau_{(k-1,l)}\right)\right]}, k > 0 \end{aligned} \tag{2}$$

where $\bar{L}$ is the average number of clusters, Λ_l is the cluster arrival rate, β is the probability controlling the particular mixture of the constituent Poisson processes and, λ_1, λ_2 are the ray arrival rates. These statistics will be used in our

simulations of Section III. We commence from the system model of Eq (1) and introduce the short-hand of:

$$C_{(k,l)} = b_{(k,l)} e^{j\phi_{(k,l)}} \quad \text{for } k = 0,1,...,K \quad l = 0,1,...,L \tag{3}$$

We continue by partitioning the system model into L number of constituent clusters of CIR taps. Each of the resultant partitions can be viewed as a constituent model characterized by a Poissonian process for each ray within that cluster, as formulated below:

$$\overbrace{C_{0,0}\delta(t-T_0-\tau_{0,0}+\ldots+C_{K,0}\delta(t-T_0-\tau_{K,0})}^{h(k,0)cluster} + \overbrace{C_{0,1}\delta(t-T_1-\tau_{0,1}+\ldots+C_{K,1}\delta(t-T_1-\tau_{K,1})}^{h(k,1)cluster} \vdots \overbrace{C_{0,L}\delta(t-T_L-\tau_{0,L}+\ldots+C_{K,L}\delta(t-T_L-\tau_{K,L})}^{h(k,L)cluster}$$

Taking the s-transform of a single constituent model yields

$$H^{(k,0)}(s) = C_{0,0}e^{-s\psi_{0,0}} + \cdots + C_{K,0}e^{-s\psi_{K,0}}, \tag{4}$$

where $\psi_{(k,l)}$ is defined as

$$\psi_{(k,l)} = T_l + \tau_{(k,l)} \quad \text{for } k = 0,1,...,K \quad l = 0,1,...,L \tag{5}$$

Using the power series expansion of $\psi_{(k,l)}$ and neglecting the higher-order terms, we have

$$e^{-s\psi_{(k,l)}} \approx 1 - s\psi_{(k,l)} \quad \text{for } k = 0,1,...,K \quad l = 0,1,...,L \tag{6}$$

Upon substituting Eq (6) into Eq (4), we obtain the transfer function of the constituent model as

$$H^{(k,0)}(s) = \left(1 - \left[\frac{\sum_{k=0}^{K} C_{k,0}\psi_{k,0}}{\sum_{k=0}^{K} C_{k,0}}\right] s\right) \sum_{k=0}^{K} C_{k,0} \tag{7}$$

The overall system transfer function can be obtained by finding and summing all the constituent transfer functions. Next, we elaborate the time domain system responses.

A. Time-Domain System Responses

The time-domain system model is obtained from Eqs (3-7) by taking the inverse s-transform, which gives

$$\left[\sum_{l=0}^{L}\sum_{k=0}^{K} b_{(k,l)} e^{j\phi_{(k,l)}}\left(T_l - \tau_{(k,l)}\right)\right]\frac{dy(t)}{dt} + \left[\sum_{l=0}^{L}\sum_{k=0}^{K} b_{(k,l)} e^{j\phi_{(k,l)}}\right] y(t) = \left[\sum_{l=0}^{L}\sum_{k=0}^{K} b_{(k,l)} e^{j\phi_{(k,l)}}\left(T_l - \tau_{(k,l)}\right)\right] Lu(t) \tag{8}$$

Where

$$u'(t) = Lu(t) \tag{9}$$

$$a^{(k,l)}(b,\phi,T,\tau) = \sum_{l=0}^{L}\sum_{k=0}^{K}\left(\frac{b_{(k,l)}e^{j\phi_{(k,l)}}}{b_{(k,l)}e^{j\phi_{(k,l)}}\left(T_l - \tau_{k,l}\right)}\right) \tag{10}$$

represents the damping coefficients, predetermining the normalized settling time of the system response. More explicitly, $a_{(k,l)}(b,\phi,T,\tau)$ is a function of the $b_{(k,l)}$, phase, cluster arrival time T and ray arrival time τ. The different model parameters were specified in [3]. More specifically, for this study we have used the so-called residential NLOS system parameters of [3].

1) Homogenous System Response

This response is obtained by substituting $u'(t)=0$ in Eq (8) and solving it for $y(t)$, which gives

$$y(t) = y(t_0)e^{-a^{(k,l)}(b,\phi,T,\tau)(t-t_0)} \quad \forall t \geq t_0 \tag{11}$$

It is readily seen in Eq (11) that the response exhibits a decaying exponent which is directly proportional to both the initial conditions at $t=t_0$ and to the damping factor $a_{(k,l)}$.

2) Non-Homogenous System Response

In order to obtain the corresponding response, we will use the general input $u'(t)$ in conjunction with an Integrating Factor (IF) of $e^{\int_{t_0}^{t}\left(a^{(k,l)}(b,\phi,T,\tau)\right)dt}$ in order to solve Eq (8), yielding the following response

$$y(t) = y(t_0)e^{-\int_{t_0}^{t}\left(a^{(k,l)}(b,\phi,T,\tau)\right)dt} + \int_{t_0}^{t} e^{-\int_{\gamma}^{t}\left(a^{(k,l)}(b,\phi,T,\tau)\right)d\xi} u'(\gamma)\,d\gamma \tag{12}$$

Upon using the short hand of

$$\theta(t,t_0) = e^{-\int_{t_0}^{t}\sum_{l=0}^{L}\sum_{k=0}^{K}\left(\frac{b_{(k,l)}e^{j\phi_{(k,l)}}}{b_{(k,l)}e^{j\phi_{(k,l)}}\left(T_l-\tau_{k,l}\right)}\right)dt}$$

$$\theta(t,\gamma) = e^{-\int_{\gamma}^{t}\sum_{l=0}^{L}\sum_{k=0}^{K}\left(\frac{b_{(k,l)}e^{j\phi_{(k,l)}}}{b_{(k,l)}e^{j\phi_{(k,l)}}\left(T_l-\tau_{k,l}\right)}\right)d\xi} \tag{13}$$

in Eq (12), we can partition the overall response into the Natural Response (N_r) and Forced Response (F_r):

$$y(t) = \underbrace{y(t_0)\theta(t,t_0)}_{N_r} + \underbrace{\int_{t_0}^{t}\theta(t,\gamma)u'(\gamma)\,d\gamma}_{F_r} \tag{14}$$

Observe in Eq (14) that N_r is dependent on the initial conditions $y(t_0)$ while F_r is directly proportional to both $u'(t)$ and to the damping parameters of Eq (13). This partitioning of the response characterizes the effect of the initial state and that of the input before reaching the steady state value. Furthermore, the partitioning in Eq (14) is also helpful in designing the rise time of the LTI system describing the UWB channel as well as its % overshoot in the transient phase.

3) Vector Form

Upon rearranging Eq (8) to give a single state-model, we arrive at:

$$\frac{dy(t)}{dt} = \frac{\left[\sum_{l=0}^{L}\sum_{k=0}^{K} b_{(k,l)}e^{j\phi_{(k,l)}}\right]}{\left[\sum_{l=0}^{L}\sum_{k=0}^{K} b_{(k,l)}e^{j\phi_{(k,l)}}\left(T_l-\tau_{(k,l)}\right)\right]} y(t) + Lu(t) \tag{15}$$

The n-state-model can be expressed from Eq (15) in a vectorial form as

$$\left[\dot{y}(t)\right]_{n\times 1} = \left[\Delta\right]_{n\times n} y(t)_{n\times 1} + \left[\chi\right]_{n\times 1} u(t)_{1\times 1} \quad (16)$$

where Δ is the system matrix of order n. By comparing Eq (8) with Eq (16), we hypothesize that the vector response of the state-model of Eq (16) is

$$y(t) = e^{\Delta(t-t_0)} y(t_0) + \int_{t_0}^{t} \left(e^{\Delta(t-\alpha)} \chi u(\alpha)\right) d\alpha \quad (17)$$

To prove this hypothesis, we need the Leibniz Integral rule (see Appendix A) and the following power series expansion

$$e^{\Delta(t-t_0)} = I + \Delta(t-t_0) + \frac{\Delta^2 (t-t_0)^2}{2!} + \ldots, \quad (18)$$

as well as its derivative given by:

$$\frac{d}{dt} e^{\Delta(t-t_0)} = \Delta + \frac{2\Delta^2 (t-t_0)}{2} + \frac{3\Delta^3 (t-t_0)}{6} + \ldots \quad (19)$$
$$= \Delta e^{\Delta(t-t_0)}$$

Check I: Substituting $t=t_0$ in the hypothesized vector response seen in Eq (17), we obtain

$$y(t)|_{t=t_0} = e^{\{0\}} y(t_0) + \overbrace{\int_{t_0}^{t_0} \left(e^{\Delta(t-\alpha)} \chi u(\alpha)\right) d\alpha}^{=0} \quad (20)$$
$$= y(t_0)$$

Check II: Taking the derivative of Eq (17), we arrive at

$$\dot{y}(t) = \Delta e^{\Delta(t-t_0)} y(t_0) + \frac{\partial}{\partial t}\left[\int_{t_0}^{t} \left(d^{\Delta(t-\alpha)} \chi u(\alpha)\right) d\alpha\right] \quad (21)$$

Applying the Leibniz integral rule (see Appendix A), we obtain

$$\dot{y}(t) = \Delta e^{\Delta(t-t_0)} y(t_0) + \Delta \int_{t_0}^{t} \left(e^{\Delta(t-\alpha)} \chi u(\alpha)\right) d\alpha \quad (22)$$
$$+ e^{\{0\}} \chi u(t) + \{0\}$$

Finally, Eq (22) can be reduced to

$$\dot{y}(t) = \Delta \overbrace{\left(e^{\Delta(t-t_0) y(t_0)} + \int_{t_0}^{t} \left(e^{\Delta(t-\alpha)} \chi u(\alpha)\right) d\alpha\right)}^{y(t)} \quad (23)$$
$$+ \chi u(t)$$

It can be seen from Eqs (20) and (23) that Eq (17) is indeed the vector response of the state-model of Eq (16).

Stability Analysis Results

This section details the step response characteristics of the LTI UWB channel derived in Section. Again, we have used the residential NLOS channel parameters of [3] stated in Table 1. Explicitly, the normalized settling time of the system is considered. Furthermore, the conditions of stability are determined for a unity feed-forward gain with the aid of Nichols chart [6].

Let us now examine Fig. 1, which portrays the LTI UWB channel's step-response on an exaggerated scale in order to facilitate this discussion. As indicated by the crosses in Fig. 1, if the damping coefficient is $a(b,\phi,T,\tau) = 1.0$, the lower limit of 0.95 is crossed when the normalized time is 4, while the upper limit of 1.05 is never crossed. A damping coefficient of $a(b,\phi,T,\tau) = 0.7$ has the lowest normalized settling time in Fig. 1, where the response crosses the −5%line at 3. Also observe in Fig. 1 that when the damping coefficient is about 0.7, the time response overshoots by almost 5%, reaching its peak after about 4.4 units of normalized time.

Table 1. Simulation parameters

Residential	NLOS
valid range of distance	7-20m
Path Gain at the reference distance G_0[dB]	-48.7
Path Gain Exponent n	4.58
Shadowing Gain S[dB]	3.51
Frequency Dependency decaying factor k	1.53
$\bar{L}$	3.5
Λ[1/ns]	0.12
λ_1, λ_2[1/ns],β	1.77, 0.15,0.045
Gamma Function Γ[ns]	26.27
Nakagami Factor m_0	0.69
Decay Time constant γ_0	17.5
Standard Deviation $\sigma_{cluster}$[dB]	2.93

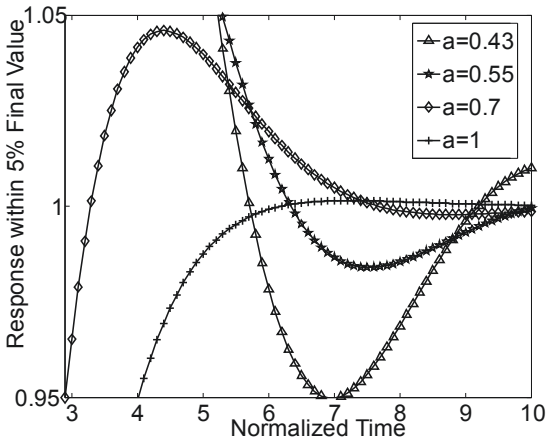

Fig. 1. Normalized step response of the LTI UWB complex channel of Eq (1) for different damping coefficient values a plotted on an expanded scale.

Let us now examine Fig. 1, which portrays the LTI UWB channel's step-response on an exaggerated scale in order to facilitate this discussion. As indicated by the crosses in Fig. 1, if the damping coefficient is $a(b,\phi,T,\tau) = 1.0$, the lower limit of 0.95 is crossed when the normalized time is 4, while the upper limit of 1.05 is never crossed. A damping coefficient of $a(b,\phi,T,\tau) = 0.7$ has the lowest normalized settling time in Fig. 1, where the response crosses the −5%line at 3. Also observe in Fig. 1 that when the damping coefficient is about 0.7, the time response overshoots by almost 5%, reaching its peak after about 4.4 units of normalized time.

As the damping coefficient drops further from 0.7 to about 0.43, the upper limit of the 5% band is entered into after the derivative has reached zero once (one extremum). However, the lower limit is never violated for a = 0.43. Since the settling-time threshold was chosen to be ±5%, the settling time is the lowest for a damping coefficient of about 0.7. The normalized settling time versus the damping coefficient relationship plotted from a range of curves such as those exemplified in Fig. 1 is seen in Fig. 2, where the different line-types indicate, which of the consecutive step-response extrema fell within the ±5% settling-time thresholds for the first time.

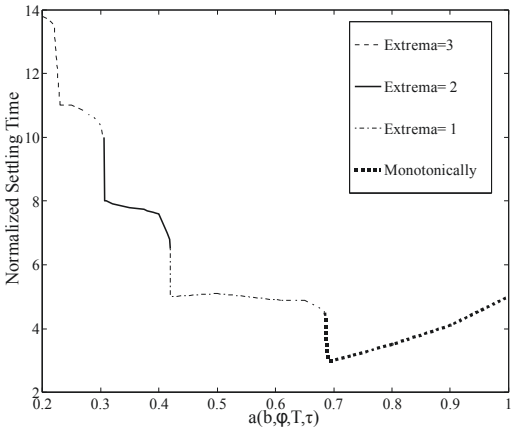

Fig. 2. Normalized Settling time of the LTI UWB channel versus the damping coefficient a of Eq (10).

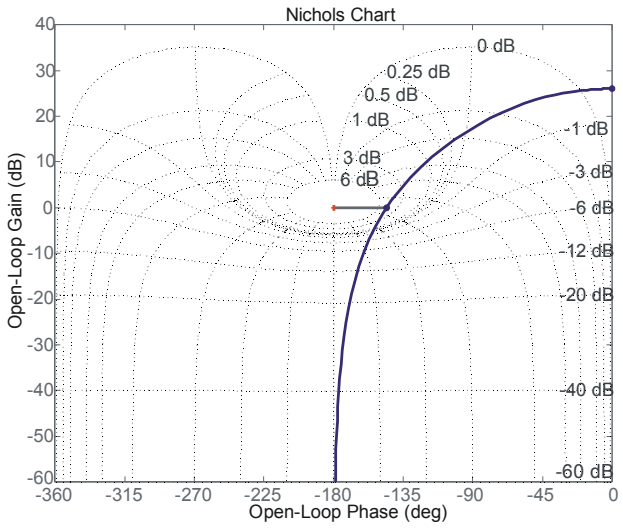

Fig. 3. Nichols Chart showing stability margins for unity feed forward gain control with parameters listed in Table 1.

The Nichols chart of Fig. 3 shows the stability margins for a unity feed-forward gain using the parameters listed in Table 1. We would like to find the specific feed-forward gain which provides a closed-loop resonance peak of 1dB. Finding the specific value of the gain which meets this specification is not as straightforward as satisfying a direct gain-margin or phase-margin specification. This is because it is not easy to locate the specific point on the original curve exemplified in Fig. 3 by inspection, which would become tangential to the required M-contour[1] of Fig. 3. We proceed by trial and error. For the design problem under consideration, the trial and error procedure gives a gain adjustment factor 8.25/20. As illustrated by Fig. 3, a peak gain of 26dB associated with the frequency of $4e^{-11}$ (rad/sec), phase margin of 34.2 degrees, delay margin of 3.19 sec with the frequency of 0.187(rad/sec) confirms closed loop stability.

Conclusion

A technique of assessing the stability of the LTI UWB channel was presented. The proposed method is based on developing closed-form analytical time-domain response expressions. The normalized settling-time and %overshoot of the step-response with respect to the damping coefficient provides a tangible metric of the system's stability. There are two important findings of the work.

1. The proposed method constitutes an alternative way of characterizing the LTI UWB channel's stability compared to the classical approach because in the classic approach it is a challenge to find all the roots of the transcendental equation in the complex s-plane.
2. This approach also provides a more convenient way of selecting the channel parameters satisfying a certain settling time, %overshoot, peak response and rise time specifications with the aid of analytical time-domain responses.

*

APPENDIX A: The Leibniz Integral General Form Differentiation under the integral sign is a useful operation in the mathematical field of calculus [5]. Explicitly, when assuming

(24) $$F(x)=\int_{a(x)}^{b(x)} f(x,t)\,dt, \quad \text{where } x_0 \le x \le x_1$$

and that if $f(x, t)$ and $\frac{\partial}{\partial t} f(x,t)$, are continuous in both t, and x, in some region of the (t, x), plane, including $a(x) \le t \le b(x)$, $x_0 \le x \le x_1$ and if $a(x)$, and $b(x)$, are continuous and have continuous derivatives for $x_0 \le x \le x_1$, then we have

(25)
$$\frac{d}{dx}F(x)=\left(\frac{\partial F}{\partial a}\right)\frac{db}{dx}-\left(\frac{\partial F}{\partial a}\right)\frac{da}{dx}+\int_{a(x)}^{b(x)}\frac{\partial}{\partial x}f(x,t)\,dt$$
$$=f\left(x,b(x)\right)b'(x)-f\left(x,a(x)\right)a'(x)+\int_{a(x)}^{b(x)}\frac{\partial}{\partial x}f(x,t)\,dt$$

for $x_0 \le x \le x_1$.

REFERENCES

[1] Yang L., Giannakis G.B.: Ultra-wideband communications: an idea whose time has come, IEEE Signal Processing Magazine, 21(6), pp. 26–54, Nov. 2004.
[2] Lopez-Salcedo J.A., Vazquez G.: Detection of PPM-UWB random signals, IEEE Trans. Signal Processing, 56(5), pp. 2003–2016, May 2008.
[3] Molisch A. F., Cassioli D., Chong C. C. and et.al.: A comprehensive standardized model for ultrawideband propagation channels, IEEE Trans. Antennas and Propagation, 54, pp. 3151–3166, 2006.
[4] Saleh A., Valenzuela R.: A statistical model for indoor multipath propagation, IEEE Journal on Selected Areas in Communications, 5(6), pp. 128–137, 1987.
[5] Flanders H.: Differentiation under the integral sign, American Mathematical Monthly, 80(2), pp. 615–627, 1973.
[6] F. M. Gardner: Phaselock techniques, Wiley, 2005.

***Authors**: prof. Ph.D. Raja A. Riaz, M. Sc. Saeed Ahmad, B.Sc. Ghufran Shafiq, Center for Advanced Studies in Telecommunication Studies (CAST), COMSATS Institute of Information Technology, Park Road, Chak Shehzad Campus, 44000,Islamabad,Pakistan,email:saeed_comsats@comsats.edu.pk ,http://cast.org.pk,email:rajaali@comsats.edu.pk,http://ciitisb.edu.pk , Ph.D. S. Chen, Ph.D. L. Hanzo, School of ECS, University of Southampton,SO171BJ,UK, http://wwwmobile.ecs.soton.ac.uk, S. Sugiura, Toyota Central Research and Development Laboratories, Japan.*

[1] Curves connecting equal values of magnitude for the closed-loop response in Nichols chart are referred to as M-contours.